research communications

A monoclinic polymorph of [(Z)-N-(3-chlorophenyl)-O-methylthiocarbamato-κS](triphenylphosphane-κP)gold(I): crystal structure and Hirshfeld surface analysis

Chien Ing Yeo, Sang Loon Tan and Edward R. T. Tiekink*

Research Centre for Crystalline Materials, Faculty of Science and Technology, Sunway University, 47500 Bandar Sunway, Selangor Darul Ehsan, Malaysia. *Correspondence e-mail: edwardt@sunway.edu.my

The title compound, [Au(C$_8$H$_7$ClNOS)(C$_{18}$H$_{15}$P)], is a monoclinic ($P2_1/n$, $Z' = 1$; form β) polymorph of the previously reported triclinic form ($P\bar{1}$, $Z' = 1$; form α) [Tadbuppa & Tiekink (2010). *Acta Cryst.* E**66**, m664]. The molecular structures of both forms feature an almost linear gold(I) coordination geometry [P—Au—S = 175.62 (5)° in the title polymorph], being coordinated by thiolate S and phosphane P atoms, a Z conformation about the C══N bond and an intramolecular Au···O contact. The major conformational difference relates to the relative orientations of the residues about the Au—S bond: the P—Au—S—C torsion angles are −8.4 (7) and 106.2 (7)° in forms α and β, respectively. The molecular packing of form β features centrosymmetric aggregates sustained by aryl-C—H···O interactions, which are connected into a three-dimensional network by aryl-C—H···π contacts. The Hirshfeld analysis of forms α and β shows many similarities with the notable exception of the influence of C—H···O interactions in form β.

1. Chemical context

Interest in the chemistry of phosphanegold(I) N-aryl-O-alkylthiocarbamates, *i.e.* compounds of general formula R_3PAu[SC(OR')══NR''] (R, R' = alkyl, aryl; R'' = aryl) continues owing to their recently disclosed exciting biological activities. Thus, various triphenylphosphane derivatives display excellent cytotoxicity profiles against HT-29 colon cancer cells, a particularly virulent form of cancer, and mechanistic studies have shown these to induce both intrinsic and extrinsic pathways of cell death leading to apoptosis (Yeo, Ooi *et al.*, 2013; Ooi *et al.*, 2015). Further, species with R'' = *p*-tolyl have proven to exhibit impressive *in vitro* potency against Gram-positive bacteria (Yeo, Sim *et al.*, 2013). It was during another synthesis of the title compound, (I), for further biological studies, that crystals of a new polymorph were isolated from its methanol solution. This is called form β to distinguish it from the earlier triclinic form, form α (Tadbuppa & Tiekink, 2010). Herein, the crystal and molecular structures of form β of (I) are described along with a comparison with the parameters characterizing form α. Further, a Hirshfeld surface analysis of both polymorphic forms of (I) is presented.
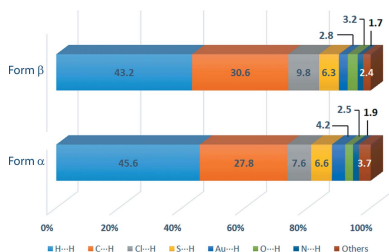
2. Structural commentary

The molecular structure of the new monoclinic form of (I), form β, is shown in Fig. 1, and selected geometric parameters

are collected in Table 1. The gold(I) atom is coordinated in an approximately linear configuration by phosphane-P and thiolate-S atoms. Confirmation of the 'thiolate' assignment is readily seen in the relatively long C1—S1 bond length and the significant π-character in the C1—N1 bond when the geometric parameters are compared with structures of related thiocarbamide molecules (Ho *et al.*, 2005; Kuan *et al.*, 2007); the crystal structure of the thiocarbamide precursor in (I) is not available for comparison. As is invariably observed in this class of compound, the Au—S bond length is longer than the Au—P bond. The small deviation from ideal linearity for the P—Au—S bond is related to the close approach of the oxygen atom to the gold(I) atom, *i.e.* 3.052 (3) Å. The pattern of bond angles about the quaternary carbon atom, C1, follow the expected trends with the widest angle involving the sulfur and doubly bonded nitrogen atom and with the narrowest angle involving the single-bonded atoms. The conformation about the formal C1=N1 bond, Table 1, is *Z*.
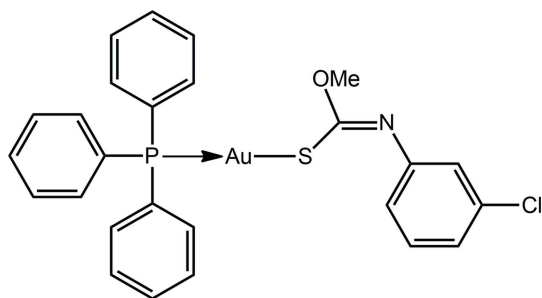
Form β crystallizes in the monoclinic space group $P2_1/n$ with $Z' = 1$. The earlier polymorph, by contrast, crystallizes in triclinic space group $P\bar{1}$, also with $Z' = 1$. A comparison of the key geometric parameters is given in Table 1. From these data, it is clear that there is experimental inequivalence in the bond lengths involving the gold(I) atoms, with the Au—S and Au—P bond lengths in form β being marginally longer. The intramolecular Au$\cdots$O separation in form β is also longer than the comparable separation in form α, and this is correlated with a smaller deviation from a linear geometry about the gold(I) atom in β. By contrast, the bond angles are, by and large, equivalent within experimental error. A significant conformational difference is evident in the molecular structures of
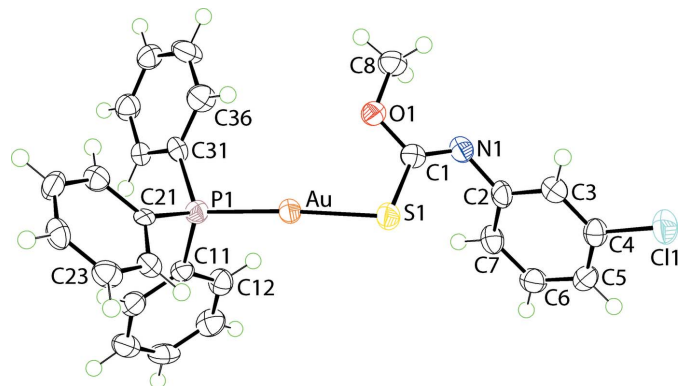
Table 1
Geometric data (Å, °) for (I), forms α^a and β, and (II)^b.

Parameter	(I): form α	(I): form β	(II)
Au—S1	2.2902 (13)	2.3070 (14)	2.3041 (9)
Au—P1	2.2416 (11)	2.2535 (14)	2.2588 (8)
C1—S1	1.760 (5)	1.764 (5)	1.759 (4)
C1—O1	1.355 (6)	1.362 (6)	1.356 (4)
C1—N1	1.241 (6)	1.274 (6)	1.265 (4)
Au$\cdots$O1	2.988 (3)	3.052 (3)	2.967 (3)
S1—Au—P1	174.61 (4)	175.62 (5)	175.86 (3)
Au—S1—C1	102.46 (16)	101.78 (18)	103.15 (12)
C1—O1—C8	116.8 (4)	115.4 (4)	117.8 (3)
C1—N1—C2	120.4 (4)	120.8 (5)	119.6 (3)
S1—C1—O1	113.0 (3)	112.6 (4)	111.9 (2)
S1—C1—N1	126.6 (4)	127.7 (4)	127.7 (3)
O1—C1—N1	120.4 (4)	119.7 (5)	120.3 (3)

Notes: (*a*) Tadbuppa & Tiekink (2010); (*b*) Tadbuppa & Tiekink (2009).

forms α and β of (I). As seen from the overlay diagram shown in Fig. 2, this difference occurs as a result of a twist about the Au—S bond as seen in the values of the P1—Au—S1—C1 torsion angles of −8.4 (7) and 106.2 (7)° in forms α and β, respectively.

3. Supramolecular features

Supramolecular dimers feature in the molecular packing of form β of (I), which are sustained by N-aryl-C—H$\cdots$O(methoxy) interactions, Fig. 3*a* and Table 2. The dimers are connected into a three-dimensional architecture by a network of C—H$\cdots\pi$ interactions, Fig. 3*b* and Table 2. Within this arrangement, centrosymmetrically related Ph$_3$P ligands align to form a so-called six-fold phenyl embrace (6PE) (Dance & Scudder, 1995) featuring edge-to-face phenyl-C—H$\cdots\pi$(phenyl) interactions, Fig. 3*c*. While the interactions are too long to be considered as significant in terms of the criteria in *PLATON* (Spek, 2009), there are a number of such interactions, *i.e.* 2 × [3.22, 3.26 and 3.29 Å], that serve to reinforce the 6PE embrace with one pair of rings accepting two interactions each. In form α of (I), the most prominent feature of the molecular packing is the formation of supramolecular chains mediated by C—H$\cdots\pi$ interactions (Tadbuppa & Tiekink, 2010). Further analysis of the molecular packing in polymorphic (I) is given in the following Section.

Figure 1
The molecular structure of polymorphic form β of (I), showing the atom-labelling scheme and displacement ellipsoids at the 70% probability level.
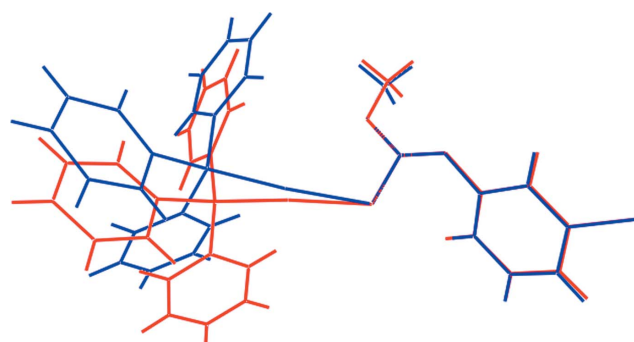
Figure 2
Overlay diagram of polymorphic forms α (blue image) and β (red) of the molecular structures of (I). Molecules have been overlapped so that the S1, O1 and N1 atoms are coincident.
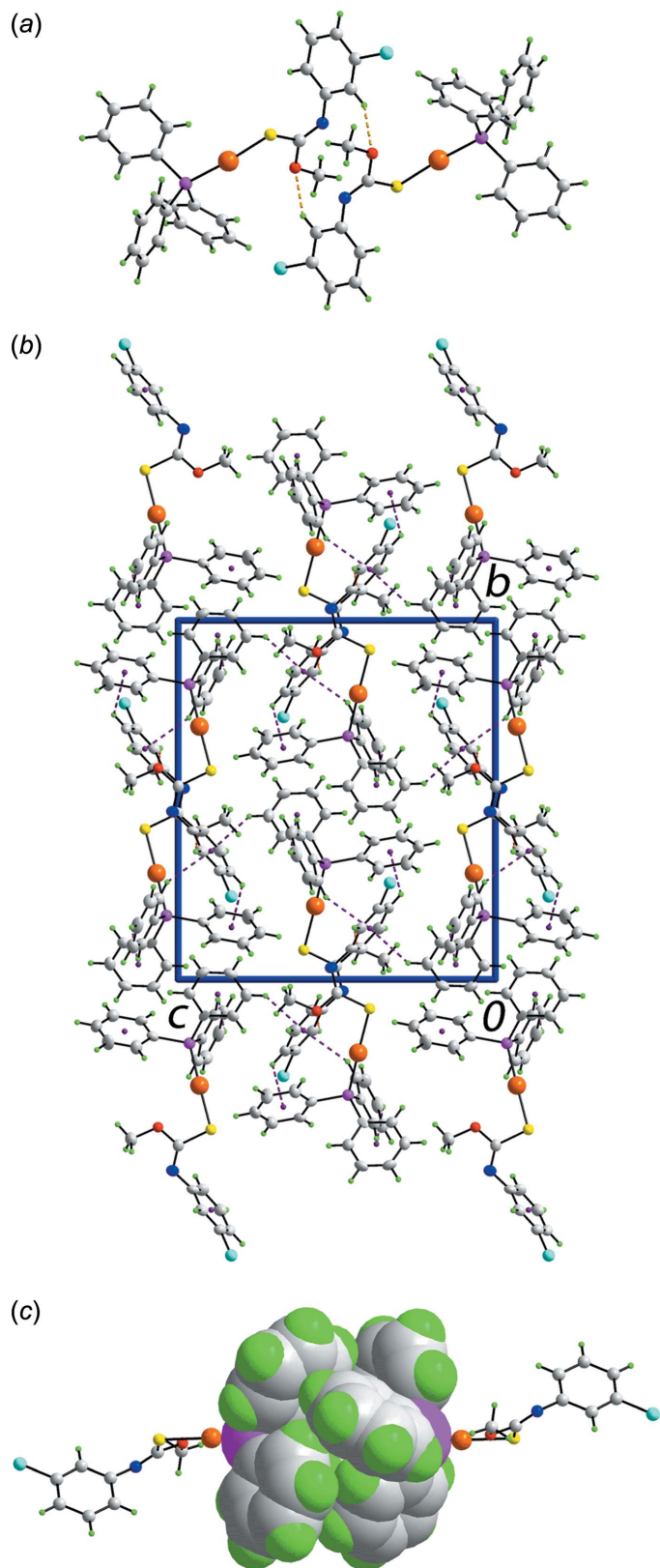
(a)

(b)

(c)

Figure 3
Molecular packing in form β of (I): (a) view of the supramolecular dimer sustained by C—H···O contacts, shown as orange dashed lines, (b) view of the unit-cell contents shown in projection down the a axis, highlighting the C—H···π interactions as purple dashed lines, (c) image of the sixfold phenyl (6PE) between centrosymmetrically related Ph$_3$P ligands, highlighted in space-filling mode.

Table 2
Hydrogen-bond geometry (Å, °).

Hydrogen-bond geometry (Å, °), form β, $Cg1$, $Cg3$ and $Cg4$ are the centroids of the C2–C7, C21–C26 and C31–C36 rings, respectively.

D—H···A	D—H	H···A	D···A	D—H···A
C3—H3···O1^{i}	0.95	2.47	3.315 (7)	148
C5—H5···$Cg4^{ii}$	0.95	2.85	3.492 (6)	126
C12—H12···$Cg1^{ii}$	0.95	2.64	3.450 (6)	143
C14—H14···$Cg3^{iii}$	0.95	2.80	3.570 (6)	139
C23—H23···$Cg1^{iv}$	0.95	2.65	3.435 (6)	140

Symmetry codes: (i) $-x + 1, -y + 2, -z + 1$; (ii) $-x, -y + 2, -z + 1$; (iii) $x - 1, y, z$; (iv) $-x + \frac{1}{2}, y - \frac{1}{2}, -z + \frac{1}{2}$.

4. Analysis of the Hirshfeld surfaces

The non-covalent interactions present in the pair of polymorphs of (I), *i.e.* forms α and β, were studied through Hirshfeld surface analysis by mapping on the normalized contact distance (d_{norm}) upon computation of the inner (d_i) and outer (d_e) distances of the Hirshfeld surface to the nearest nucleus (Spackman & Jayatilaka, 2009; McKinnon *et al.*, 2007). All computation as well as generation of two-dimensional fingerprint plots were performed using *Crystal Explorer 3.1* (Wolff *et al.*, 2012). Distances involving hydrogen atoms were normalized by default to the standard neutron-diffraction bond lengths.

As evident from Fig. 4 and Table 3, forms α and β of (I) exhibit relatively similar percentage contributions of the indicated intermolecular interactions to their Hirshfeld surfaces. However, the specific contributions to their interaction profiles are distinct as evidenced from the overall and decomposed two-dimensional fingerprint plots shown in Fig. 5. As mentioned above in *Supramolecular features*, C—H···π interactions feature in both structures. To a first approximation the decomposed fingerprint plots look similar, as seen from Fig. 5b. However, relatively shorter contacts are found in form β *cf.* form α, *i.e.* 2.62 *vs* 2.68 Å. The clear distinction between the two forms is readily noted from the decomposed fingerprint plots for the O···H/H···O contacts with very
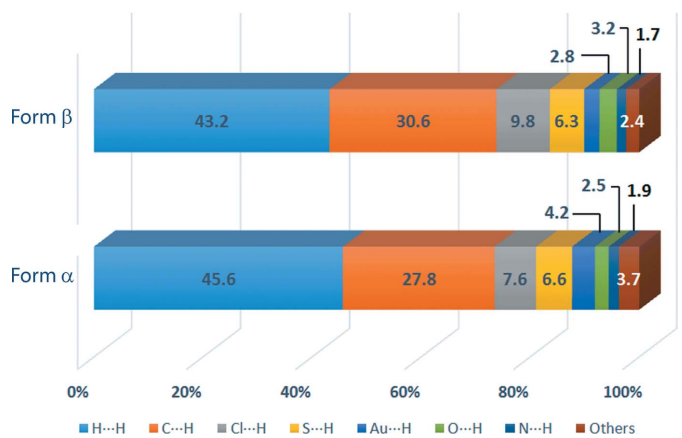
Figure 4
Percentage contribution of different close contacts to the Hirshfeld surface of forms α and β of (I).

distinct spikes evident for form β, Fig. 5c, correlating with the C—H···O interactions leading to dimer formation. While beyond the sum of their respective van der Waals radii (Spek, 2009), Cl···H/H···Cl interactions make contributions to the Hirshfeld surfaces of both forms α and β, with the contacts, again, being shorter in form β, i.e. 2.76 vs 3.00 Å, leading to more the distinct forceps in Fig. 5d.

In general, the observation of generally shorter contacts in form β may indicate greater crystal-packing efficiency (Lloyd et al., 2005). Table 4 collates various molecular/crystal structure descriptors for the polymorphic forms. Immediately evident is that the calculated unit-cell densities are identical but the crystal-packing efficiency (KPI; Spek, 2009) for form β is marginally greater. Computation on the area-to-volume ratio between forms α and β revealed very little difference as did the globularity (G) and asphericity (Ω) indices. All these indicators suggest that the polymorphs arise as a result of a simple interplay between molecular conformation and crystal-packing effects.

5. Database survey

The most closely related structure to (I) in the crystallographic literature (Groom et al., 2016), is the $R' = $ OEt analogue, i.e. (II), (Tadbuppa & Tiekink, 2009). Key geometric parameters for this structure are also included in Table 1. Non-systematic variations in parameters are noted, e.g. the Au—S bond length in (II) is intermediate between those found in the polymorphic forms of (I), and the Au—P bond length is the longest of the three structures. However, differences are small and probably can be ascribed to the influences of crystal-packing effects.
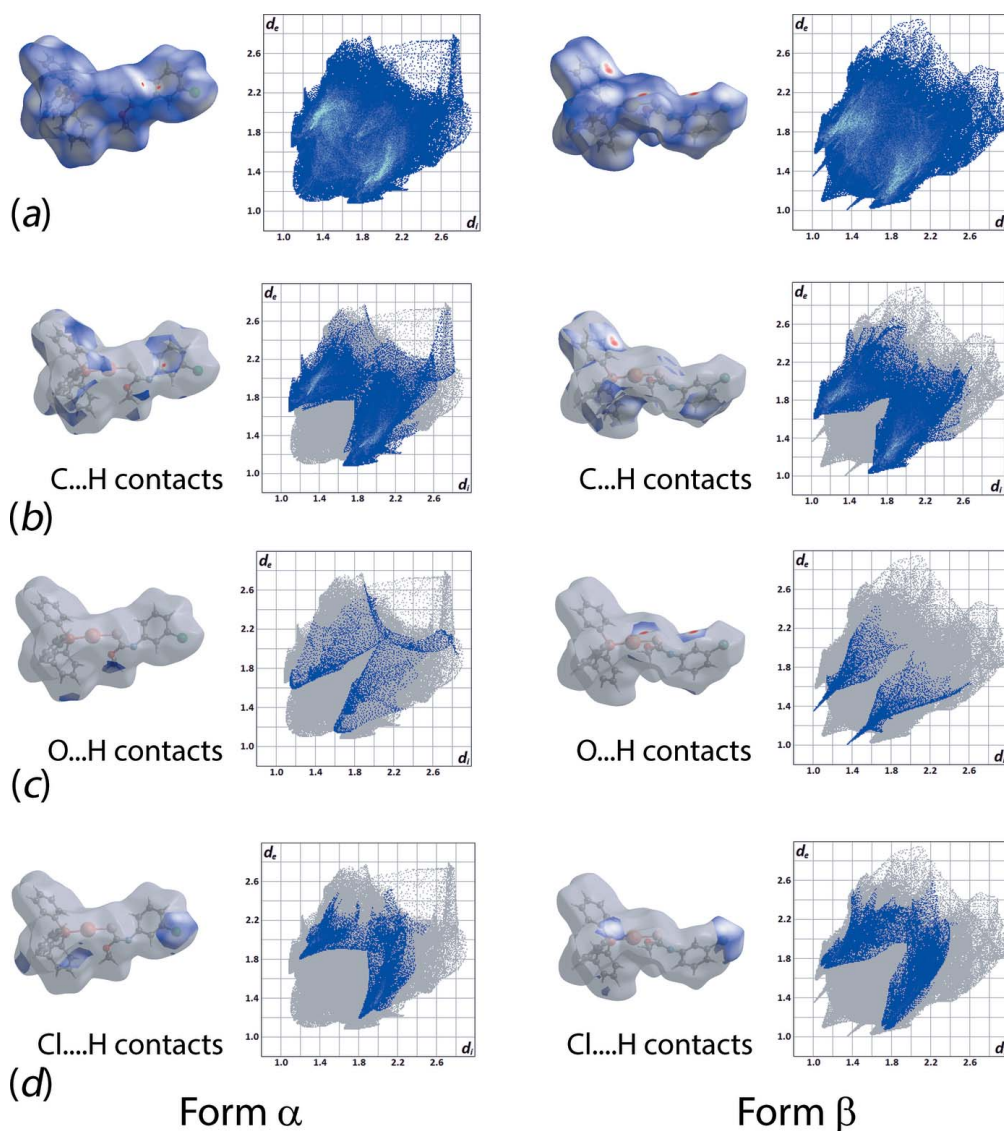

Figure 5
Comparison of the (a) complete Hirshfeld surface and full fingerprint plots between form α and form β polymorphs (top row) and the corresponding d_{norm} surfaces and two-dimensional plots associated with (b) C···H/H···C, (c) O···H/H···O and (d) Cl···H/H···Cl contacts.

Table 3
Percentage contribution of the different intermolecular contacts to the Hirshfeld surface in forms α and β of (I).

Contact	% Contribution form α	% Contribution form β
Au···Cl	0.2	0.6
Au···C	0.3	0.2
Au···H	4.2	2.8
Cl···C	2.7	0.3
Cl···H	7.6	9.8
Cl···S	0.0	0.2
S···C	0.1	0.0
S···H	6.6	6.3
O···H	2.5	3.2
N···H	1.9	1.7
N···C	0.0	0.3
C···C	0.4	0.8
C···H	27.8	30.6
H···H	45.6	43.2
Total	99.9	100

Table 4
Physiochemical properties for forms α and β of (I).

Parameter	Form α	Form β
Volume, V (Å^3)	596.42	596.78
Surface area, A (Å^2)	518.92	511.11
A:V (Å^{-1})	0.87	0.86
Globularity, G	0.660	0.671
Asphericity, Ω	0.165	0.172
Density (g cm^{-1})	1.805	1.805
Packing index (%)	66.9	67.4

Table 5
Experimental details.

Crystal data	
Chemical formula	[Au(C$_8$H$_7$ClNOS)(C$_{18}$H$_{15}$P)]
M_r	659.89
Crystal system, space group	Monoclinic, $P2_1/n$
Temperature (K)	100
a, b, c (Å)	9.0078 (4), 17.4732 (7), 15.5641 (7)
β (°)	97.595 (4)
V (Å^3)	2428.22 (18)
Z	4
Radiation type	Mo $K\alpha$
μ (mm^{-1})	6.34
Crystal size (mm)	0.10 × 0.05 × 0.03
Data collection	
Diffractometer	Agilent SuperNova Dual Source diffractometer with an Atlas detector
Absorption correction	Multi-scan (*CrysAlis PRO*; Agilent, 2010)
T_{min}, T_{max}	0.570, 0.833
No. of measured, independent and observed [$I > 2\sigma(I)$] reflections	18211, 5613, 4470
R_{int}	0.065
$(\sin \theta/\lambda)_{max}$ (Å^{-1})	0.651
Refinement	
$R[F^2 > 2\sigma(F^2)]$, $wR(F^2)$, S	0.040, 0.090, 1.05
No. of reflections	5613
No. of parameters	290
H-atom treatment	H-atom parameters constrained
$\Delta\rho_{max}$, $\Delta\rho_{min}$ (e Å^{-3})	2.04, −1.06

Computer programs: *CrysAlis PRO* (Agilent, 2010), *SHELXS97* (Sheldrick, 2008), *SHELXL2014* (Sheldrick, 2015), *ORTEP-3 for Windows* (Farrugia, 2012), *QMol* (Gans & Shalloway, 2001), *DIAMOND* (Brandenburg, 2006) and *publCIF* (Westrip, 2010).

As indicated in the *Chemical context*, biological considerations motivate ongoing investigations into the chemistry of phosphanegold(I) *N*-aryl-*O*-alkylthiocarbamates. This notwithstanding, the relative ease of growing crystals have prompted several crystal engineering studies. Thus, correlations between Au···Au (aurophilic) and solid-state luminescence responses have been made for the series of compounds, R_3PAu[SC(OMe)=NC$_6$H$_4$NO$_2$-p] (R = Et, Cy and Ph), and bidentate phosphane analogues, Ph$_2$P–(CH$_2$)$_n$–PPh$_2$ for n = 1–4 and when the bridge is Fc (ferrocenyl) (Ho *et al.*, 2006). In another study, the influence of R and Y substituents upon the molecular packing of compounds of the general formula [(Ph$_2$P(CH$_2$)$_4$PPh$_2$){AuSC(OR')=NC$_6$H$_4$Y-p}$_2$] for R' = Me, Et or iPr and Y = H, NO$_2$ or Me was undertaken (Ho & Tiekink, 2007). Besides the anticipated linear P—Au—S configuration, a common feature of all the analysed structures until then was the presence of intramolecular Au···O interactions, as illustrated in Fig. 1. This changed in another systematic study, this time of R_3PAu[SC(OMe)=NR''], for R = Ph, *o*-tol, *m*-tol or *p*-tol, and R'' = Ph, *o*-tol, *m*-tol, *p*-tol or C$_6$H$_4$NO$_2$-p, where it proved possible to induce a conformational change in the molecule so that an intramolecular Au···π interaction formed rather than Au···O (Kuan *et al.*, 2008); Au···π interactions are well documented in the crystallographic literature (Tiekink & Zukerman-Schpector, 2009; Caracelli *et al.*, 2013). For example, having R = R'' = *p*-tol simultaneously activated the gold atom, making it amenable to form an Au···π interaction with the comparatively electron-rich aryl ring. Recently, bipodal forms of the thiocarbamide ligands were prepared and complexed with phosphanegold(I) species yielding binuclear molecules also with intramolecular Au···π interactions (Yeo *et al.*, 2015). Computational chemistry showed the Au···π interactions to be more favourable, by *ca* 12 kcal mol^{-1}, than the putative Au···O interaction (Yeo *et al.*, 2015).

Such interplay between substituents in crystal engineering endeavours, along with the observation that biological activities are acutely sensitive to substitution patterns, ensures this area of research will continue to attract significant attention.

6. Synthesis and crystallization

All chemicals and solvents were used as purchased without purification. All reactions were carried out under ambient conditions. Melting points were determined on a Biobase auto melting point apparatus MP300. IR spectra were obtained on a Perkin Elmer Spectrum 400 FT Mid-IR/Far-IR spectrophotometer from 4000 to 400 cm^{-1}; abbreviation: s, strong.

Preparation of (I): NaOH (Merck; 0.25 mmol, 0.01 g) in MeOH (Merck; 1 ml) was added to a suspension of Ph$_3$PAuCl (0.25 mmol, 0.12 g) in MeOH (Merck; 15 ml), followed by addition of the thiocarbamide, MeOC(=S)N(H)C$_6$H$_4$Cl$_3$ (0.25 mmol, 0.05 g), prepared following literature precedents (Ho *et al.*, 2005), in MeOH (15 ml). The resulting mixture was stirred for 2 h at 323 K. The solution mixture was left for slow

evaporation at room temperature, yielding colourless prisms of the title compound after 3 weeks. Yield: 0.134 g (81%). M.p. 431–433 K. IR (cm^{-1}): 1434 (*s*) ν(C=N), 1180 (*s*) ν(C—O), 1098 (*s*) ν(C—S).

7. Refinement

Crystal data, data collection and structure refinement details are summarized in Table 5. The carbon-bound H atoms were placed in calculated positions (C—H = 0.95–0.98 Å) and were included in the refinement in the riding-model approximation, with U_{iso}(H) set to 1.2–1.5U_{eq}(C). The maximum and minimum residual electron density peaks of 2.04 and 1.06 e Å^{-3}, respectively, were located 1.01 and 0.77 Å from the Au atom.

References

Agilent (2010). *CrysAlis PRO*. Agilent Technologies Inc., Santa Clara, CA, USA.

Brandenburg, K. (2006). *DIAMOND*. Crystal Impact GbR, Bonn, Germany.

Caracelli, I., Zukerman-Schpector, J. & Tiekink, E. R. T. (2013). *Gold Bull.* **46**, 81–89.

Dance, I. & Scudder, M. (1995). *J. Chem. Soc. Chem. Commun.* pp. 1039–1040.

Farrugia, L. J. (2012). *J. Appl. Cryst.* **45**, 849–854.

Gans, J. & Shalloway, D. (2001). *J. Mol. Graphics Modell.* **19**, 557–559.

Groom, C. R., Bruno, I. J., Lightfoot, M. P. & Ward, S. C. (2016). *Acta Cryst.* B**72**, 171–179.

Ho, S. Y., Bettens, R. P. A., Dakternieks, D., Duthie, A. & Tiekink, E. R. T. (2005). *CrystEngComm*, **7**, 682–689.

Ho, S. Y., Cheng, E. C.-C., Tiekink, E. R. T. & Yam, V. W.-W. (2006). *Inorg. Chem.* **45**, 8165–8174.

Ho, S. Y. & Tiekink, E. R. T. (2007). *CrystEngComm*, **9**, 368–378.

Kuan, F. S., Mohr, F., Tadbuppa, P. P. & Tiekink, E. R. T. (2007). *CrystEngComm*, **9**, 574–581.

Kuan, F. S., Ho, S. Y., Tadbuppa, P. P. & Tiekink, E. R. T. (2008). *CrystEngComm*, **10**, 548–564.

Lloyd, G. O., Bredenkamp, M. W. & Barbour, L. J. (2005). *Chem. Commun.* pp. 4053–4055.

McKinnon, J. J., Jayatilaka, D. & Spackman, M. A. (2007). *Chem Commun.* pp. 3814–3816.

Ooi, K. K., Yeo, C. I., Ang, K.-P., Akim, A. Md., Cheah, Y.-K., Halim, S. N. A., Seng, H.-L. & Tiekink, E. R. T. (2015). *J. Biol. Inorg. Chem.* **20**, 855–873.

Sheldrick, G. M. (2008). *Acta Cryst.* A**64**, 112–122.

Sheldrick, G. M. (2015). *Acta Cryst.* C**71**, 3–8.

Spackman, M. A. & Jayatilaka, D. (2009). *CrystEngComm*, **11**, 19–32.

Spek, A. L. (2009). *Acta Cryst.* D**65**, 148–155.

Tadbuppa, P. P. & Tiekink, E. R. T. (2009). *Acta Cryst.* E**65**, m1663.

Tadbuppa, P. P. & Tiekink, E. R. T. (2010). *Acta Cryst.* E**66**, m664.

Tiekink, E. R. T. & Zukerman-Schpector, J. (2009). *CrystEngComm*, **11**, 1176–1186.

Westrip, S. P. (2010). *J. Appl. Cryst.* **43**, 920–925.

Wolff, S. K., Grimwood, D. J., McKinnon, J. J., Turner, M. J., Jayatilaka, D. & Spackman, M. A. (2012). *Crystal Explorer*. The University of Western Australia.

Yeo, C. I., Khoo, C.-H., Chu, W.-C., Chen, B-J., Chu, P.-L., Sim, J.-H., Cheah, Y.-K., Ahmad, J., Halim, S. N. A., Seng, H.-L., Ng, S., Otero-de-la-Roza, A. & Tiekink, E. R. T. (2015). *RSC Adv.* **5**, 41401–41411.

Yeo, C. I., Ooi, K. K., Akim, A. Md., Ang, K. P., Fairuz, Z. A., Halim, S. N. B. A., Ng, S. W., Seng, H.-L. & Tiekink, E. R. T. (2013). *J. Inorg. Biochem.* **127**, 24–38.

Yeo, C. I., Sim, J.-H., Khoo, C.-H., Goh, Z.-J., Ang, K.-P., Cheah, Y.-K., Fairuz, Z. A., Halim, S. N. B. A., Ng, S. W., Seng, H.-L. & Tiekink, E. R. T. (2013). *Gold Bull.* **46**, 145–152.

supporting information

A monoclinic polymorph of [(*Z*)-*N*-(3-chlorophenyl)-*O*-methylthiocarbamato-*κS*](triphenylphosphane-*κP*)gold(I): crystal structure and Hirshfeld surface analysis

Chien Ing Yeo, Sang Loon Tan and Edward R. T. Tiekink

Computing details

Data collection: *CrysAlis PRO* (Agilent, 2010); cell refinement: *CrysAlis PRO* (Agilent, 2010); data reduction: *CrysAlis PRO* (Agilent, 2010); program(s) used to solve structure: *SHELXS97* (Sheldrick, 2008); program(s) used to refine structure: *SHELXL2014* (Sheldrick, 2015); molecular graphics: *ORTEP-3 for Windows* (Farrugia, 2012), *QMol* (Gans & Shalloway, 2001) and *DIAMOND* (Brandenburg, 2006); software used to prepare material for publication: *publCIF* (Westrip, 2010).

[(*Z*)-*N*-(3-Chlorophenyl)-*O*-methylthiocarbamato-*κS*](triphenylphosphane-*κP*)gold(I)

Crystal data

[Au(C$_8$H$_7$ClNOS)(C$_{18}$H$_{15}$P)]	$F(000) = 1280$
$M_r = 659.89$	$D_x = 1.805$ Mg m^{-3}
Monoclinic, $P2_1/n$	Mo $K\alpha$ radiation, $\lambda = 0.71073$ Å
$a = 9.0078$ (4) Å	Cell parameters from 5344 reflections
$b = 17.4732$ (7) Å	$\theta = 2.3$–27.5°
$c = 15.5641$ (7) Å	$\mu = 6.34$ mm^{-1}
$\beta = 97.595$ (4)°	$T = 100$ K
$V = 2428.22$ (18) Å^3	Prism, colourless
$Z = 4$	$0.10 \times 0.05 \times 0.03$ mm

Data collection

Agilent SuperNova Dual Source diffractometer with an Atlas detector	$T_{min} = 0.570$, $T_{max} = 0.833$
	18211 measured reflections
Radiation source: SuperNova (Mo) X-ray Source	5613 independent reflections
	4470 reflections with $I > 2\sigma(I)$
Mirror monochromator	$R_{int} = 0.065$
Detector resolution: 10.4041 pixels mm^{-1}	$\theta_{max} = 27.6°$, $\theta_{min} = 2.3°$
ω scan	$h = -11 \rightarrow 9$
Absorption correction: multi-scan (CrysAlis PRO; Agilent, 2010)	$k = -22 \rightarrow 22$
	$l = -17 \rightarrow 20$

Refinement

Refinement on F^2	290 parameters
Least-squares matrix: full	0 restraints
$R[F^2 > 2\sigma(F^2)] = 0.040$	Hydrogen site location: inferred from neighbouring sites
$wR(F^2) = 0.090$	
$S = 1.05$	H-atom parameters constrained
5613 reflections	

$w = 1/[\sigma^2(F_o^2) + (0.0282P)^2]$
where $P = (F_o^2 + 2F_c^2)/3$
$(\Delta/\sigma)_{max} < 0.001$

$\Delta\rho_{max} = 2.04$ e Å^{-3}
$\Delta\rho_{min} = -1.06$ e Å^{-3}

Special details

Geometry. All esds (except the esd in the dihedral angle between two l.s. planes) are estimated using the full covariance matrix. The cell esds are taken into account individually in the estimation of esds in distances, angles and torsion angles; correlations between esds in cell parameters are only used when they are defined by crystal symmetry. An approximate (isotropic) treatment of cell esds is used for estimating esds involving l.s. planes.

Fractional atomic coordinates and isotropic or equivalent isotropic displacement parameters (Å^2)

	x	*y*	*z*	U_{iso}*/U_{eq}
Au	0.19155 (2)	0.79563 (2)	0.43242 (2)	0.02135 (8)
Cl1	0.35621 (18)	1.26890 (8)	0.33228 (10)	0.0342 (4)
P1	0.11209 (17)	0.67786 (8)	0.46382 (9)	0.0209 (3)
S1	0.25415 (18)	0.91846 (8)	0.39637 (9)	0.0263 (3)
O1	0.3390 (4)	0.9118 (2)	0.5632 (2)	0.0231 (8)
N1	0.2776 (5)	1.0330 (2)	0.5172 (3)	0.0238 (10)
C1	0.2894 (6)	0.9623 (3)	0.4991 (3)	0.0206 (11)
C2	0.2162 (7)	1.0859 (3)	0.4530 (4)	0.0240 (12)
C3	0.3063 (6)	1.1426 (3)	0.4247 (3)	0.0222 (12)
H3	0.4107	1.1438	0.4442	0.027*
C4	0.2408 (7)	1.1975 (3)	0.3675 (4)	0.0237 (12)
C5	0.0901 (7)	1.1990 (3)	0.3373 (4)	0.0231 (12)
H5	0.0489	1.2371	0.2975	0.028*
C6	0.0000 (7)	1.1425 (3)	0.3670 (4)	0.0270 (13)
H6	−0.1046	1.1423	0.3478	0.032*
C7	0.0618 (6)	1.0863 (3)	0.4249 (4)	0.0262 (13)
H7	−0.0007	1.0484	0.4452	0.031*
C8	0.3796 (7)	0.9450 (3)	0.6480 (3)	0.0294 (13)
H8A	0.4077	0.9042	0.6903	0.044*
H8B	0.2941	0.9735	0.6647	0.044*
H8C	0.4645	0.9798	0.6466	0.044*
C11	−0.0850 (6)	0.6656 (3)	0.4249 (3)	0.0208 (12)
C12	−0.1829 (7)	0.7251 (3)	0.4386 (4)	0.0258 (13)
H12	−0.1448	0.7711	0.4657	0.031*
C13	−0.3350 (7)	0.7173 (3)	0.4127 (4)	0.0316 (14)
H13	−0.4014	0.7575	0.4228	0.038*
C14	−0.3908 (7)	0.6504 (3)	0.3719 (4)	0.0301 (14)
H14	−0.4953	0.6451	0.3544	0.036*
C15	−0.2952 (7)	0.5923 (3)	0.3569 (4)	0.0289 (13)
H15	−0.3340	0.5474	0.3277	0.035*
C16	−0.1436 (6)	0.5982 (3)	0.3838 (3)	0.0252 (12)
H16	−0.0788	0.5569	0.3747	0.030*
C21	0.2049 (5)	0.6011 (3)	0.4174 (3)	0.0157 (11)
C22	0.2091 (6)	0.6018 (3)	0.3269 (3)	0.0222 (12)
H22	0.1637	0.6431	0.2935	0.027*
C23	0.2778 (6)	0.5437 (3)	0.2856 (4)	0.0261 (13)

H23	0.2804	0.5458	0.2248	0.031*
C24	0.3423 (6)	0.4830 (3)	0.3338 (4)	0.0251 (12)
H24	0.3879	0.4427	0.3057	0.030*
C25	0.3412 (6)	0.4803 (3)	0.4227 (4)	0.0258 (13)
H25	0.3868	0.4386	0.4554	0.031*
C26	0.2729 (6)	0.5389 (3)	0.4639 (4)	0.0243 (12)
H26	0.2725	0.5366	0.5248	0.029*
C31	0.1333 (6)	0.6589 (3)	0.5800 (3)	0.0197 (11)
C32	0.0283 (6)	0.6151 (3)	0.6158 (3)	0.0233 (12)
H32	−0.0569	0.5951	0.5804	0.028*
C33	0.0503 (7)	0.6009 (3)	0.7051 (4)	0.0274 (13)
H33	−0.0207	0.5709	0.7303	0.033*
C34	0.1734 (7)	0.6299 (3)	0.7572 (4)	0.0293 (14)
H34	0.1883	0.6192	0.8176	0.035*
C35	0.2751 (7)	0.6748 (3)	0.7201 (4)	0.0318 (14)
H35	0.3587	0.6961	0.7557	0.038*
C36	0.2558 (7)	0.6890 (3)	0.6314 (4)	0.0286 (13)
H36	0.3265	0.7192	0.6063	0.034*

Atomic displacement parameters (Å^2)

	U^{11}	U^{22}	U^{33}	U^{12}	U^{13}	U^{23}
Au	0.02540 (14)	0.01827 (12)	0.02023 (13)	−0.00202 (8)	0.00242 (9)	−0.00004 (8)
Cl1	0.0355 (9)	0.0266 (7)	0.0414 (9)	−0.0078 (6)	0.0081 (7)	0.0040 (6)
P1	0.0232 (8)	0.0201 (7)	0.0192 (7)	0.0002 (6)	0.0027 (6)	0.0008 (5)
S1	0.0387 (9)	0.0204 (7)	0.0198 (7)	−0.0048 (6)	0.0033 (6)	0.0002 (5)
O1	0.025 (2)	0.022 (2)	0.022 (2)	0.0015 (16)	0.0009 (16)	−0.0001 (15)
N1	0.023 (3)	0.021 (2)	0.027 (3)	−0.0022 (19)	0.003 (2)	−0.0017 (19)
C1	0.018 (3)	0.024 (3)	0.020 (3)	−0.002 (2)	0.004 (2)	0.000 (2)
C2	0.031 (3)	0.014 (3)	0.026 (3)	−0.001 (2)	0.004 (2)	−0.003 (2)
C3	0.020 (3)	0.022 (3)	0.025 (3)	0.002 (2)	0.004 (2)	−0.005 (2)
C4	0.026 (3)	0.020 (3)	0.026 (3)	0.000 (2)	0.007 (2)	−0.001 (2)
C5	0.031 (3)	0.020 (3)	0.019 (3)	0.006 (2)	0.005 (2)	0.000 (2)
C6	0.026 (3)	0.026 (3)	0.028 (3)	0.002 (2)	−0.002 (2)	−0.003 (2)
C7	0.024 (3)	0.023 (3)	0.033 (3)	−0.005 (2)	0.006 (3)	0.000 (2)
C8	0.033 (4)	0.030 (3)	0.023 (3)	0.001 (3)	−0.001 (3)	−0.003 (2)
C11	0.023 (3)	0.022 (3)	0.016 (3)	−0.002 (2)	0.001 (2)	0.002 (2)
C12	0.029 (3)	0.023 (3)	0.025 (3)	0.002 (2)	0.006 (3)	−0.002 (2)
C13	0.030 (4)	0.034 (3)	0.032 (3)	0.009 (3)	0.005 (3)	0.000 (3)
C14	0.019 (3)	0.046 (4)	0.023 (3)	−0.006 (3)	−0.004 (2)	0.004 (3)
C15	0.029 (3)	0.033 (3)	0.023 (3)	−0.005 (3)	0.000 (2)	−0.003 (2)
C16	0.024 (3)	0.024 (3)	0.026 (3)	0.001 (2)	0.000 (2)	0.004 (2)
C21	0.007 (3)	0.019 (3)	0.019 (3)	−0.009 (2)	−0.005 (2)	0.006 (2)
C22	0.022 (3)	0.021 (3)	0.023 (3)	−0.003 (2)	0.001 (2)	−0.003 (2)
C23	0.028 (3)	0.031 (3)	0.020 (3)	−0.005 (3)	0.004 (2)	−0.002 (2)
C24	0.025 (3)	0.018 (3)	0.032 (3)	0.002 (2)	0.006 (2)	−0.006 (2)
C25	0.027 (3)	0.019 (3)	0.030 (3)	0.002 (2)	0.001 (3)	0.007 (2)
C26	0.027 (3)	0.024 (3)	0.022 (3)	−0.001 (2)	0.002 (2)	−0.002 (2)

C31	0.020 (3)	0.016 (3)	0.023 (3)	−0.002 (2)	0.005 (2)	−0.005 (2)
C32	0.027 (3)	0.015 (3)	0.026 (3)	−0.002 (2)	−0.003 (2)	0.000 (2)
C33	0.031 (3)	0.026 (3)	0.026 (3)	−0.001 (3)	0.005 (3)	0.002 (2)
C34	0.039 (4)	0.026 (3)	0.021 (3)	0.001 (3)	0.000 (3)	0.003 (2)
C35	0.030 (4)	0.040 (3)	0.024 (3)	−0.013 (3)	−0.004 (3)	−0.002 (3)
C36	0.031 (4)	0.033 (3)	0.023 (3)	−0.004 (3)	0.006 (3)	0.001 (2)

Geometric parameters (Å, º)

Au—P1	2.2535 (14)	C13—H13	0.9500
Au—S1	2.3070 (14)	C14—C15	1.372 (8)
Cl1—C4	1.756 (6)	C14—H14	0.9500
P1—C21	1.783 (5)	C15—C16	1.378 (8)
P1—C11	1.811 (6)	C15—H15	0.9500
P1—C31	1.824 (5)	C16—H16	0.9500
S1—C1	1.764 (5)	C21—C26	1.402 (7)
O1—C1	1.362 (6)	C21—C22	1.413 (7)
O1—C8	1.443 (6)	C22—C23	1.390 (7)
N1—C1	1.274 (6)	C22—H22	0.9500
N1—C2	1.418 (7)	C23—C24	1.383 (7)
C2—C3	1.389 (8)	C23—H23	0.9500
C2—C7	1.402 (8)	C24—C25	1.386 (8)
C3—C4	1.387 (7)	C24—H24	0.9500
C3—H3	0.9500	C25—C26	1.394 (7)
C4—C5	1.378 (8)	C25—H25	0.9500
C5—C6	1.395 (8)	C26—H26	0.9500
C5—H5	0.9500	C31—C36	1.379 (7)
C6—C7	1.398 (7)	C31—C32	1.389 (7)
C6—H6	0.9500	C32—C33	1.399 (7)
C7—H7	0.9500	C32—H32	0.9500
C8—H8A	0.9800	C33—C34	1.380 (8)
C8—H8B	0.9800	C33—H33	0.9500
C8—H8C	0.9800	C34—C35	1.389 (8)
C11—C12	1.398 (8)	C34—H34	0.9500
C11—C16	1.409 (7)	C35—C36	1.391 (8)
C12—C13	1.383 (8)	C35—H35	0.9500
C12—H12	0.9500	C36—H36	0.9500
C13—C14	1.391 (8)		
P1—Au—S1	175.62 (5)	C15—C14—C13	120.2 (6)
C21—P1—C11	105.5 (2)	C15—C14—H14	119.9
C21—P1—C31	105.8 (2)	C13—C14—H14	119.9
C11—P1—C31	106.2 (2)	C14—C15—C16	120.8 (5)
C21—P1—Au	114.80 (17)	C14—C15—H15	119.6
C11—P1—Au	111.17 (17)	C16—C15—H15	119.6
C31—P1—Au	112.75 (17)	C15—C16—C11	119.8 (5)
C1—S1—Au	101.78 (18)	C15—C16—H16	120.1
C1—O1—C8	115.4 (4)	C11—C16—H16	120.1

C1—N1—C2	120.8 (5)	C26—C21—C22	117.0 (5)
N1—C1—O1	119.7 (5)	C26—C21—P1	124.8 (4)
N1—C1—S1	127.7 (4)	C22—C21—P1	118.2 (4)
O1—C1—S1	112.6 (4)	C23—C22—C21	121.8 (5)
C3—C2—C7	119.6 (5)	C23—C22—H22	119.1
C3—C2—N1	119.9 (5)	C21—C22—H22	119.1
C7—C2—N1	120.1 (5)	C24—C23—C22	119.4 (5)
C4—C3—C2	118.8 (5)	C24—C23—H23	120.3
C4—C3—H3	120.6	C22—C23—H23	120.3
C2—C3—H3	120.6	C23—C24—C25	120.6 (5)
C5—C4—C3	123.2 (5)	C23—C24—H24	119.7
C5—C4—Cl1	118.5 (4)	C25—C24—H24	119.7
C3—C4—Cl1	118.2 (4)	C24—C25—C26	119.8 (5)
C4—C5—C6	117.6 (5)	C24—C25—H25	120.1
C4—C5—H5	121.2	C26—C25—H25	120.1
C6—C5—H5	121.2	C25—C26—C21	121.5 (5)
C5—C6—C7	120.8 (5)	C25—C26—H26	119.3
C5—C6—H6	119.6	C21—C26—H26	119.3
C7—C6—H6	119.6	C36—C31—C32	120.8 (5)
C6—C7—C2	119.9 (5)	C36—C31—P1	118.4 (4)
C6—C7—H7	120.0	C32—C31—P1	120.7 (4)
C2—C7—H7	120.0	C31—C32—C33	118.8 (5)
O1—C8—H8A	109.5	C31—C32—H32	120.6
O1—C8—H8B	109.5	C33—C32—H32	120.6
H8A—C8—H8B	109.5	C34—C33—C32	121.0 (5)
O1—C8—H8C	109.5	C34—C33—H33	119.5
H8A—C8—H8C	109.5	C32—C33—H33	119.5
H8B—C8—H8C	109.5	C33—C34—C35	119.1 (5)
C12—C11—C16	119.0 (5)	C33—C34—H34	120.5
C12—C11—P1	118.1 (4)	C35—C34—H34	120.5
C16—C11—P1	122.9 (4)	C34—C35—C36	120.7 (5)
C13—C12—C11	120.2 (5)	C34—C35—H35	119.7
C13—C12—H12	119.9	C36—C35—H35	119.7
C11—C12—H12	119.9	C31—C36—C35	119.5 (5)
C12—C13—C14	120.0 (6)	C31—C36—H36	120.2
C12—C13—H13	120.0	C35—C36—H36	120.2
C14—C13—H13	120.0		
C2—N1—C1—O1	−175.5 (5)	C12—C11—C16—C15	0.8 (8)
C2—N1—C1—S1	6.8 (8)	P1—C11—C16—C15	179.0 (4)
C8—O1—C1—N1	−2.1 (7)	C11—P1—C21—C26	−110.0 (5)
C8—O1—C1—S1	176.0 (4)	C31—P1—C21—C26	2.3 (5)
Au—S1—C1—N1	−153.4 (5)	Au—P1—C21—C26	127.3 (4)
Au—S1—C1—O1	28.7 (4)	C11—P1—C21—C22	69.0 (4)
C1—N1—C2—C3	−113.5 (6)	C31—P1—C21—C22	−178.7 (4)
C1—N1—C2—C7	73.4 (7)	Au—P1—C21—C22	−53.7 (4)
C7—C2—C3—C4	−1.4 (8)	C26—C21—C22—C23	−0.2 (7)
N1—C2—C3—C4	−174.6 (5)	P1—C21—C22—C23	−179.3 (4)

C2—C3—C4—C5	0.3 (8)	C21—C22—C23—C24	0.8 (8)	
C2—C3—C4—Cl1	−180.0 (4)	C22—C23—C24—C25	−1.1 (8)	
C3—C4—C5—C6	0.7 (8)	C23—C24—C25—C26	0.7 (8)	
Cl1—C4—C5—C6	−179.0 (4)	C24—C25—C26—C21	−0.1 (8)	
C4—C5—C6—C7	−0.6 (8)	C22—C21—C26—C25	−0.2 (8)	
C5—C6—C7—C2	−0.6 (8)	P1—C21—C26—C25	178.8 (4)	
C3—C2—C7—C6	1.6 (8)	C21—P1—C31—C36	90.7 (5)	
N1—C2—C7—C6	174.7 (5)	C11—P1—C31—C36	−157.5 (4)	
C21—P1—C11—C12	−169.0 (4)	Au—P1—C31—C36	−35.5 (5)	
C31—P1—C11—C12	79.0 (5)	C21—P1—C31—C32	−89.3 (5)	
Au—P1—C11—C12	−44.0 (5)	C11—P1—C31—C32	22.4 (5)	
C21—P1—C11—C16	12.7 (5)	Au—P1—C31—C32	144.4 (4)	
C31—P1—C11—C16	−99.3 (5)	C36—C31—C32—C33	−1.1 (8)	
Au—P1—C11—C16	137.7 (4)	P1—C31—C32—C33	179.0 (4)	
C16—C11—C12—C13	0.6 (8)	C31—C32—C33—C34	0.2 (8)	
P1—C11—C12—C13	−177.7 (4)	C32—C33—C34—C35	1.1 (9)	
C11—C12—C13—C14	−0.8 (9)	C33—C34—C35—C36	−1.7 (9)	
C12—C13—C14—C15	−0.3 (9)	C32—C31—C36—C35	0.6 (9)	
C13—C14—C15—C16	1.7 (9)	P1—C31—C36—C35	−179.5 (5)	
C14—C15—C16—C11	−1.9 (8)	C34—C35—C36—C31	0.8 (9)	

Hydrogen-bond geometry (Å, °)

Hydrogen-bond geometry (Å, °) for (I), Form *β*, *Cg*1, *Cg*3 and *Cg*4 are the centroids of the C2–C7, C21–C26 and C31–C36 rings, respectively.

D—H⋯*A*	*D*—H	H⋯*A*	*D*⋯*A*	*D*—H⋯*A*
C3—H3⋯O1[i]	0.95	2.47	3.315 (7)	148
C5—H5⋯*Cg*4[ii]	0.95	2.85	3.492 (6)	126
C12—H12⋯*Cg*1[ii]	0.95	2.64	3.450 (6)	143
C14—H14⋯*Cg*3[iii]	0.95	2.80	3.570 (6)	139
C23—H23⋯*Cg*1[iv]	0.95	2.65	3.435 (6)	140

Symmetry codes: (i) −*x*+1, −*y*+2, −*z*+1; (ii) −*x*, −*y*+2, −*z*+1; (iii) *x*−1, *y*, *z*; (iv) −*x*+1/2, *y*−1/2, −*z*+1/2.